

# Local thermal non-equilibrium in sediments: Implications for temperature dynamics and the use of heat as a tracer

Roshan, H.; Cuthbert, Mark; Andersen, M.S.; Acworth, R.I.

DOI:

[10.1016/j.advwatres.2014.08.002](https://doi.org/10.1016/j.advwatres.2014.08.002)

License:

Other (please specify with Rights Statement)

*Document Version*

Peer reviewed version

*Citation for published version (Harvard):*

Roshan, H, Cuthbert, M, Andersen, MS & Acworth, RI 2014, 'Local thermal non-equilibrium in sediments: Implications for temperature dynamics and the use of heat as a tracer', *Advances in Water Resources*, vol. 73, pp. 176-184. <https://doi.org/10.1016/j.advwatres.2014.08.002>

[Link to publication on Research at Birmingham portal](#)

## **Publisher Rights Statement:**

NOTICE: this is the author's version of a work that was accepted for publication in *Advances in Water Resources*. Changes resulting from the publishing process, such as peer review, editing, corrections, structural formatting, and other quality control mechanisms may not be reflected in this document. Changes may have been made to this work since it was submitted for publication. A definitive version was subsequently published in *Advances in Water Resources* [VOL 73, November 2014] DOI: 10.1016/j.advwatres.2014.08.002

Eligibility for repository checked October 2014

## **General rights**

Unless a licence is specified above, all rights (including copyright and moral rights) in this document are retained by the authors and/or the copyright holders. The express permission of the copyright holder must be obtained for any use of this material other than for purposes permitted by law.

- Users may freely distribute the URL that is used to identify this publication.
- Users may download and/or print one copy of the publication from the University of Birmingham research portal for the purpose of private study or non-commercial research.
- User may use extracts from the document in line with the concept of 'fair dealing' under the Copyright, Designs and Patents Act 1988 (?)
- Users may not further distribute the material nor use it for the purposes of commercial gain.

Where a licence is displayed above, please note the terms and conditions of the licence govern your use of this document.

When citing, please reference the published version.

## **Take down policy**

While the University of Birmingham exercises care and attention in making items available there are rare occasions when an item has been uploaded in error or has been deemed to be commercially or otherwise sensitive.

If you believe that this is the case for this document, please contact [UBIRA@lists.bham.ac.uk](mailto:UBIRA@lists.bham.ac.uk) providing details and we will remove access to the work immediately and investigate.

## Accepted Manuscript

Local thermal non-equilibrium in sediments: implications for temperature dynamics and the use of heat as a tracer

H. Roshan, M.O. Cuthbert, M.S. Andersen, R.I. Acworth

PII: S0309-1708(14)00155-9

DOI: <http://dx.doi.org/10.1016/j.advwatres.2014.08.002>

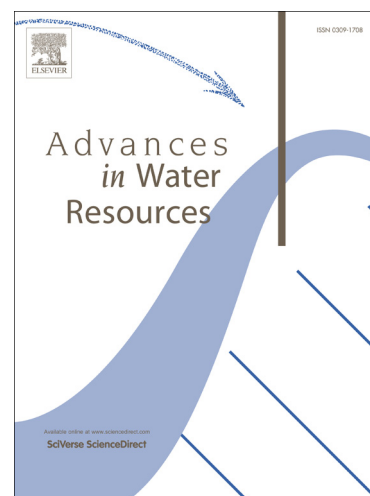
Reference: ADWR 2249

To appear in: *Advances in Water Resources*

Received Date: 28 January 2014

Revised Date: 23 June 2014

Accepted Date: 2 August 2014



Please cite this article as: Roshan, H., Cuthbert, M.O., Andersen, M.S., Acworth, R.I., Local thermal non-equilibrium in sediments: implications for temperature dynamics and the use of heat as a tracer, *Advances in Water Resources* (2014), doi: <http://dx.doi.org/10.1016/j.advwatres.2014.08.002>

This is a PDF file of an unedited manuscript that has been accepted for publication. As a service to our customers we are providing this early version of the manuscript. The manuscript will undergo copyediting, typesetting, and review of the resulting proof before it is published in its final form. Please note that during the production process errors may be discovered which could affect the content, and all legal disclaimers that apply to the journal pertain.

1 **Local thermal non-equilibrium in sediments: implications for temperature dynamics**  
2 **and the use of heat as a tracer**

3 Corresponding author: H. Roshan, Connected Waters Initiative Research Centre, University  
4 of New South Wales, 110 King St, Manly Vale, NSW 2093, Australia and National Centre  
5 for Groundwater Research and Training, Australia  
6 h.roshan@unsw.edu.au

7 M. O. Cuthbert, Connected Waters Initiative Research Centre, University of New South  
8 Wales and Water Sciences (Hydrogeology), School of Geography, Earth and Environmental  
9 Sciences, University of Birmingham, UK

10 M. S. Andersen, Connected Waters Initiative Research Centre, University of New South  
11 Wales and National Centre for Groundwater Research and Training, Australia

12 R. I. Acworth, Connected Waters Initiative Research Centre, University of New South Wales  
13 and National Centre for Groundwater Research and Training, Australia

14

15

16

17

18

19

20

21

22

23

24

25

26

27

28

29

30

31

32

33

## 34 **Abstract**

35 Understanding streambed thermal processes is of fundamental importance due to the effects of  
36 temperature dynamics on stream ecology and solute exchange processes. Local Thermal  
37 Equilibrium (LTE) between fluid and solid is usually assumed for modelling heat exchange in  
38 streambeds and for inferring pore water flow velocities from streambed temperature data. By  
39 examining well established experimental and theoretical relationships of the fluid-solid heat  
40 transfer coefficient in a numerical scheme for a range of Reynolds ( $Re$ ) numbers ( $0.01 > Re >$   
41  $0.001$ ), we show here that, for a range of typical streambed conditions, LTE is not attained. Thus  
42 errors in velocity estimates obtained when inverting streambed temperature data assuming LTE  
43 can be considerable especially at relatively low flow rates. We show that for certain conditions  
44 where the LTE assumption is not valid, inferred pore water velocities of up to 1 m/d can be  
45 obtained with LTE assumption even if the actual velocities are much smaller or even zero.  
46 Ignoring the possibility of Local Thermal Non-Equilibrium (LTNE) will have consequences for  
47 the correct estimation of streambed pore water and heat fluxes at low  $Re$  values. More  
48 laboratory studies are urgently needed to supplement the sparse existing data in this area and  
49 further test the findings of this study.

50 *Keywords: Local thermal non-equilibrium, Heat as a tracer, Heat transfer, streambed*

51

## 52 **1. Introduction**

53 Understanding streambed temperature dynamics is critical to deriving deeper insights into  
54 stream ecology. Temperature is a fundamental biological variable and is a major control on  
55 biogeochemical processes which underpin vital ecosystem services [1]. Moreover,  
56 measurements of temperature variability between streams and groundwater [2] can be used to  
57 infer patterns and processes of hyporheic exchange [3] and are critical for controlling nutrient  
58 and carbon cycling in streambed systems and the potential attenuation of contaminants in the  
59 hyporheic zone [4]. Most techniques which use heat as a tracer rely on a physically based  
60 model which inverts temperature measurements to infer flow rates and sediment thermal  
61 properties [5]. The most popular methods take advantage of the solar signal which generally  
62 induces heat exchange between streams and underlying sediments [6-9]. A damping and  
63 attenuation of the diel stream temperature signal with depth is normally observed and most  
64 methods assume a 1-D flow field for interpretation, although recent studies have shown that this

65 may be problematic in real, non-uniform, flow fields [10, 11]. Additional uncertainties may  
 66 stem from sediment heterogeneity [12], measurement error and difficulties in estimating thermal  
 67 parameters [13, 14].

68 Despite its increasing popularity in the hydrological community, all studies to date which have  
 69 used heat as a tracer for investigating groundwater-surface water interactions in streambed  
 70 environments have assumed the validity of the single-temperature (i.e. using a single domain to  
 71 model temperatures for the solid and fluid in combination) heat transport equation. This relies  
 72 on the assumption of instantaneous local thermal equilibrium between the solid matrix materials  
 73 and the pore fluids. However, we show here, by drawing on the extensive literature on this  
 74 subject from other fields and proposing a new correlation, that this assumption is questionable in  
 75 the context of many streambeds. As a result, considerable errors in flux estimation and  
 76 conceptual understanding of streambed thermal processes may result.

77

## 78 **2. Methods**

### 79 **2.1 Deriving the heat transfer coefficient at low Reynolds numbers typical of streambeds**

80 When the assumption of LTE is suspected to break down, the temperature of solid and fluid  
 81 phases have to be considered separately rather than as a single average temperature field. In this  
 82 two-domain approach, it is assumed that each phase is continuous and represented by an  
 83 appropriate effective total thermal conductivity and therefore effective thermal diffusivity [15,  
 84 16]. We use a *Dispersion-Particle-Based* two-equation model based on the heat transfer  
 85 coefficient between the solid and the fluid phases. The equations for the solid and the fluid  
 86 phases without heat sources or sinks and without an energy term for viscous-work can be  
 87 expressed as [17, 18]:

$$88 \quad \frac{\partial T^f}{\partial t} + v \frac{\partial T^f}{\partial x} = \frac{1}{\phi} \left( \frac{k_f}{(\rho c_p)_f} + f \left( \bar{\beta}, \bar{v} \right) \right) \frac{\partial^2 T^f}{\partial x^2} + \frac{h_{sf} a_{sf}}{\phi (\rho c_p)_f} (T^s - T^f) \quad (1)$$

$$89 \quad \frac{\partial T^s}{\partial t} = \frac{k_s}{(1-\phi)(\rho c_p)_s} \frac{\partial^2 T^s}{\partial x^2} - \frac{h_{sf} a_{sf}}{(1-\phi)(\rho c_p)_s} (T^s - T^f) \quad (2)$$

90 Where,  $a_{sf}$  is the surface area of particle per unit volume of porous media,  $h_{sf}$  is the heat  
 91 transfer coefficient,  $\phi$  is the overall porosity and  $k$  is the thermal conductivity tensor,  
 92 respectively where  $f$  represents the fluid phase and  $s$  represent the solid phase. Also  $(\rho c_p)_f$  is

93 the volumetric heat capacity of fluid,  $(\rho c_p)_s$  is the volumetric heat capacity of solid,  $T^f$  is the

94 fluid temperature,  $T^s$  is the solid temperature and  $t$  is the time. In addition  $f(\vec{\beta}, \vec{v})$  is the

95 hydrodynamic dispersion function:  $f(\vec{\beta}, \vec{v}) = \vec{\beta} \cdot \left( \frac{\rho_f c_f}{\rho c} \cdot \vec{v} \right)^2$  proposed by Rau et al. [19]

96 where  $\vec{\beta}$  is the thermal dispersivity matrix and  $\vec{v}$  is the average pore water velocity defined as a  
97 vector. In this form of the hydrodynamic dispersion function the thermal dispersivity has the  
98 units of [T]. In Eqs. 1 and 2, the surface area of particles per unit volume of porous media can be  
99 estimated by [20]:

$$100 \quad a_{sf} = \frac{6(1-\phi)}{dp} \quad (3)$$

101 Where,  $dp$  is defined as the average grain size of the porous media as would be obtained from a  
102 grain size distribution curve. It should be noted that this equation may not be valid for poorly  
103 sorted sediment, but is applicable to the homogeneous conditions modelled here. In order to  
104 determine the heat transfer coefficient between the fluid and solid particles, a number of  
105 experimental correlations have been proposed [21-23]. However, despite extensive effort, no  
106 theory has been developed which can satisfactorily describe the heat transfer rate over a wide  
107 range of porous media with different physical properties, such as grain size or velocity  
108 distribution [21]. At high Reynolds numbers, there is a well-accepted correlation which has  
109 been used to solve the heat transfer in porous beds for more than three decades. It is expressed  
110 as [21]:

$$111 \quad Nu = 2 + 1.1 Pr^{\frac{1}{3}} Re^{0.6} \quad (4)$$

112 where,  $Nu$ ,  $Pr$  and  $Re$  are the dimensionless Nusselt number, Prandtl number and Reynolds  
113 number defined as:

$$114 \quad Nu = \frac{h_s dp}{k_f}, \quad Pr = \frac{c_{pf} \mu_f}{k_f}, \quad Re = \frac{\rho_f v dp}{\mu_f} \quad (5)$$

115 where,  $\mu_f$ ,  $c_{pf}$  and  $\rho_f$  are the fluid viscosity, fluid heat capacity and fluid density. Increase in  
116  $Re$  enhances heat and momentum transfer between fluid particles which increases the friction

117 force on the grain surface and therefore the heat transfer rate. The average grain thermal Peclet  
 118 number ( $Pe_{avg}$ ) describes the ratio of the advective to conductive heat transport and defined as:

$$119 \quad Pe_{avg} = \frac{\rho_f c_{pf} v dp}{k_e} \quad (6)$$

120 where,  $k_e$  is the average heat conductivity of the porous medium defined as  $k_e = k_s^{(1-\phi)} \cdot k_f^{(\phi)}$ . The  
 121 proposed correlation (equation 4) explains the experimental data obtained by many authors [24,  
 122 25] for  $Re > 1$ . However, such high  $Re$  are not expected in streambeds unless the grainsize and  
 123 thus hydraulic conductivity of the bed are sufficiently great and large hydraulic gradients are  
 124 also present to drive high fluid velocities such as might be the case in high energy losing stream  
 125 systems [26]. For example, a gravel streambed with an average grainsize of 1 mm and a pore-  
 126 water velocity of 10 m/d would have a  $Re$  of around 0.1 ( $Pe_{avg} = 0.074$  when  $k_s = 2.5 \text{ W(mC)}^{-1}$ ).  
 127 However, many streambed environments have smaller grain sizes (silt to sand i.e. 0.01 mm to  
 128 1 mm) or smaller pore water velocities due to lower ambient hydraulic gradients such as are  
 129 often found in lowland settings [7, 14, 27] leading to relatively low Reynolds numbers. For  
 130 example a sandy streambed ( $dp = 0.3 \text{ mm}$ ) with a pore water velocity of around 0.3 m/d would  
 131 have a  $Re$  of approximately 0.001 ( $Pe_{avg} = 7.4 \times 10^{-4}$  when  $k_s = 2.5 \text{ W(mC)}^{-1}$ ).

132 For  $Re < 1$  relevant to many streambed environments, fewer data are available and equation (4)  
 133 breaks down. Therefore, we propose a correlation based on the only experimental data  
 134 published to date [28] to calculate the heat transfer coefficient at low Reynolds numbers (down  
 135 to  $Re = 0.001$ ). These data have been widely used in various studies in the literature [22, 29, 30].  
 136 In order to obtain a correlation of the heat transfer in saturated sand, only the part of the Kunii  
 137 and Smith [28] data related to experimentation with water as the fluid phase and sand and glass  
 138 beads (with thermal conductivity of  $0.5 \text{ W(mC)}^{-1}$ ) as the solid phase were plotted and analysed  
 139 (**Figure 1**). The mathematical equation explaining the physics of heat transfer of a single sphere  
 140 submerged in a fluid is used as the basis of the analysis [31]:

$$141 \quad Nu = 2.0 + K_1 Pr^p Re^q \quad (7)$$

142 where,  $K_1$ ,  $p$  and  $q$  are experimental coefficients. It is discussed in Nelson and Galloway [22]  
 143 that the coefficient of 2 in equation (7) is only valid for single sphere and this coefficient needs  
 144 to be measured experimentally for real materials. It is also shown by Lienhard [32] that the ratio  
 145 of thickness of the thermal boundary layer  $\delta_t$  to that of the fluid boundary layer  $\delta_f$  equals to:

146  $\frac{\delta_t}{\delta_f} = \text{Pr}^{-\frac{1}{3}}$  for a wide range of gas and fluids  $0.6 \leq \text{Pr} \leq 50$ . Thus, in derivation of the heat  
 147 transfer equation the Prandtl number takes the power of 1/3. Therefore, we would expect  
 148 equation (7) to take the following form:

$$149 \quad Nu = \alpha + K_1 \text{Pr}^{\frac{1}{3}} \text{Re}^q \quad (8)$$

150 We used the software *Datafit* to fit equation (8) to the Kunii and Smith [28] experimental data  
 151 by varying the parameters  $\alpha$ ,  $K_1$  and  $q$  by a least squares method. The coefficients were  
 152 chosen from the best fit (details of fitting parameters and confidence intervals can be found in  
 153 Table A and B in Appendix A). In addition, the model proposed by Nelson and Galloway [22] is  
 154 also considered to compare the results of each model at  $Re=0.01$ . The Nelson and Galloway  
 155 model has been widely used in the industry applications having Reynolds numbers down to 0.01  
 156 [33, 34]. The model has the form:

$$157 \quad Nu = \frac{2\zeta + \left( \frac{2\zeta^2(1-\phi)^{1/3}}{[1-(1-\phi)^{1/3}]^2} - 2 \right) \tanh \zeta}{\frac{\zeta}{1-(1-\phi)^{1/3}} - \tanh \zeta} \quad (9)$$

$$158 \quad \text{where, } \zeta = 0.3 \left[ \frac{1}{(1-\phi)^{1/3}} - 1 \right] \text{Re}^{1/2} \text{Pr}^{1/3}.$$

159 Presented in Figure 1 are also the curves of Nusselt number versus Reynolds numbers for  
 160 different porosities based on the model of Nelson and Galloway [22]. It is worth noting that the  
 161 system of one sphere grain in a fluid is assumed to have the porosity of 1. The Nelson and  
 162 Galloway curves of Figure 1 therefore represent natural sediments at lower to intermediate  
 163 porosities and at a porosity of 1 the extreme case of heat transfer between fluid and a single  
 164 sphere.

165

## 166 **2.2 Forward two-domain numerical model**

167 Both the proposed correlation based on the Kunii and Smith [28] data and Nelson and Galloway  
 168 [22] theory were embedded into a finite element numerical code to forward model the two-  
 169 temperature equations (1 & 2) for physical parameters typical of streambed materials [11] (also  
 170 shown in Table 1). In the analysis,  $Pe$  was varied by changing the pore water velocity ( $\sim 0.01$ ,



171 0.04, 0.09 and 0.3 m/d) and solid thermal conductivity (the upper and lower bound of thermal  
172 conductivity of solids are  $k_{s\_min} = 0.8 \text{ W(mC)}^{-1}$  and  $k_{s\_max} = 2.5 \text{ W(mC)}^{-1}$ ) [35]. While we  
173 recognise that this velocity range is at the lower end for typical streambeds, using realistic  
174 thermal properties it is as high a range as is possible while staying within the  $Re$  range of of the  
175 Kunii and Smith [28] data on which our heat transfer correlation is based.

176 For a particular combination of parameters, equations 8 & 9 were solved for  $Nu$  and then  $h_{sf}$  was  
177 extracted from equation 5 and used in equations 1 & 2. In order to solve Eqs. 1 and 2  
178 simultaneously, the initial fluid temperature was used to calculate the solid temperature with the  
179 obtained heat transfer coefficient. The obtained solid temperature is then used to calculate new  
180 fluid temperature. The  $i^{\text{th}}$ -step fluid temperature was then compared with  $i-1^{\text{th}}$  step fluid  
181 temperature using a least square technique to check the convergence. The convergence is  
182 considered satisfied for a temperature error of 0.01 °C. A two dimensional mesh with 21 nodes  
183 along x-axis (0.1 m) and 8421 nodes along y axis (4.0 m) with 10 mins time steps were used in  
184 the numerical simulation. The depth of 4 m to the lower boundary was sufficient to not influence  
185 the results extracted from the upper 0.45 m used for the analysis.

186 Standard Galerkin and Characteristic Galerkin Finite Element discretization techniques [36, 37]  
187 with a least square method were used to simultaneously solve for solid and fluid temperatures  
188 (equations 1 & 2). Natural heat convection due to buoyancy effects was neglected assuming  
189 that the forced convection dominates the heat transfer process [17]. It is also noteworthy that,  
190 for the range of  $Re$  investigated in this study, the thermal dispersion was negligible [19].

191 Since most studies of groundwater-surface water interactions using heat as a tracer focus on diel  
192 temperature signals, we used a daily sinusoidal upper temperature boundary condition for all  
193 model scenarios on top and a constant temperature boundary condition (25°C) at the bottom and  
194 no flow boundaries at the sides. The initial temperature across the whole model domain was  
195 25°C. An amplitude of 4°C for the top boundary starting at 25°C (i.e.  $T_0 = T_{ave}$ ) was used for all  
196 runs except for one case where sensitivity to the amplitude was tested. A steady state downward  
197 fluid flow was assumed and basic physical parameters typical of streambed materials [11] were  
198 used. Fluid velocity was varied across a range typically found in the streambed environment for  
199  $0.001 < Re < 0.01$ . However the heat transfer coefficient used for the analysis was not extrapolated  
200 lower than the lower end of  $Re$  numbers from the Kunii and Smith [28] experimental data. This

201 prevents from extracting a superficial magnitude for heat transfer coefficient at very low  
 202 Reynolds numbers ( $Re < 0.001$ ). Models were run for 100 days and the output from the last day  
 203 of each run was analysed. The finite element numerical discretization of the governing equations  
 204 (1 & 2) is presented in Appendix B.

205

### 206 **2.3 Inverse single-domain analytical model**

207 The output from the two-domain forward models was used as ‘synthetic field data’ and the  
 208 amplitude ratios ( $AR$ ) and phase shifts ( $PS$ ) of the temperature signal with depth were calculated  
 209 relative to the upper temperature boundary condition. In a theoretical sense, the fluid and solid  
 210 temperatures define the upper and lower range of temperature that probes might monitor in  
 211 streambeds depending on the relative size of the temperature monitoring device and the grain  
 212 size of the streambed material. In reality, temperature probes will integrate temperature  
 213 responses from the fluid and solid. However for this analysis, rather than choosing an arbitrary  
 214 averaging of temperatures which would be site-dependent varying with the type of field  
 215 instrument used and streambed material, we inverted the data for the fluid and solid separately  
 216 to show the maximum differences that could arise. Therefore, to represent this range within the  
 217 synthetic data derived from the forward models,  $ARs$  and  $PSs$  were calculated for the individual  
 218 temperatures of the fluid ( $T_f$ ) and solid ( $T_s$ ) phases throughout the analysis. The  $AR$  and  $PS$   
 219 values were then inverted using the commonly used equation which assumes LTE [6] via the  
 220 equations proposed by Hatch et al. [8] (and the ‘known’ porosity and thermal parameters in the  
 221 forward model) to produce values of pore water velocity at depths of 0.1, 0.2, 0.3, 0.35, 0.4 and  
 222 0.45 m. Errors in fluid velocity were calculated by comparing the inverse model results with  
 223 those used in the forward models. For the inversions the bulk thermal diffusivity,  $D$ , was  
 224 assumed to be given by the following average of the solid and fluid phases:

$$225 \quad D_{avg} = \frac{(1-\phi)k_s + \phi k_f}{(1-\phi)(\rho c_p)_s + \phi(\rho c_p)_f}$$

226 In this bulk averaging, the fluid and solid phases are considered as parallel resistors allowing the  
 227 calculation of the overall energy flux through the system.

228

## 229 **3. Results and Discussion**

### 230 **3.1 Heat transfer coefficients for low Reynolds numbers**

231 The best fit correlation of equation (8) to the Kunii and Smith [28] data takes the form:

$$232 \quad Nu = 2.4 \times 10^{-5} + 285.6 Pr^{\frac{1}{3}} Re^{2.7} \quad (10)$$

233 The correlation is shown against the data in Figure 1 alongside output from the Nelson-  
 234 Galloway Model (NGM). For the modelled porosity of 0.3 used here, the agreement between  
 235 the Kunii and Smith Correlation (KSC) and the NGM is good for practical applications at  
 236  $Re=0.01$  where the ranges of applicability overlap. This gives confidence in the approach taken  
 237 here for estimating the heat transfer coefficient. Note that the curves shown for the highest  
 238 porosities are unrealistic for natural materials but can be realistic for heat transfer within loosely  
 239 packed beds used in chemical reactors. One sphere grain is assumed to have a porosity of 1 and  
 240 therefore the curves with higher porosity approach the case of heat transfer between fluid and a  
 241 single sphere.

242

### 243 **3.2 Simulated local thermal non-equilibrium between solid and fluid phases for sinusoidal** 244 **varying temperature input**

245 Marked differences, up to approximately 1 °C in the modelled cases, were found between the  
 246 solid and fluid phase temperatures derived from the two-domain model at a range of depths and  
 247  $Pe$  (and  $Re$ ) with a surface temperature amplitude of 4 °C and solid thermal conductivity of  
 248 either 0.8 or 2.5 W(mC)<sup>-1</sup>. **Figure 2** illustrates this for a depth of 0.2 m and for high and low  $Re$   
 249 ( $2.5 \times 10^{-4}$  and  $7.5 \times 10^{-3}$ ). The figure also includes the case with thermal equilibrium (e.g. the  
 250 Hatch equation [8]) and the purely conductive case for comparison. At the low  $Re$  of  $2.5 \times 10^{-4}$   
 251 the purely conductive case and the LTE case are producing almost identical temperature  
 252 fluctuations at 0.2 m depth. This illustrates that for this low  $Re$  identifying a velocity different  
 253 from zero probably leads to inaccuracy. However, for the two-domain model the temperature  
 254 fluctuations for solid and fluid differ from each other as well as from the conductive and the  
 255 LTE cases (both in terms of amplitude and phase). It is interesting to note that the temperature  
 256 fluctuations for the solid and fluid cannot be combined (by some weighed average) to produce  
 257 the one-domain analytical LTE temperature fluctuations since they are both simultaneously  
 258 lower (or both higher) than the LTE temperature. At higher  $Re$  ( $=7.5 \times 10^{-3}$ ), there is now a  
 259 distinct difference between the conductive case and the LTE case. However, the temperature of  
 260 fluid and solid from the two-domain model and LTE case are almost identical for high and low

261 solid thermal conductivities showing that the two-domain system is approaching thermal  
262 equilibrium.

263 We extracted the difference between the sinusoid amplitude of the solid and fluid temperatures  
264 (ATD) as a measure of the thermal disequilibrium. In order to investigate the effect of change in  
265 amplitude of surface temperature on ATD at different Reynolds numbers, four temperature  
266 sinusoids with amplitude of 1, 2, 3 and 4°C were applied on the surface boundary (**Figure 3**)  
267 and the response was measured at 0.2 m depth. In this analysis, the volumetric heat transfer  
268 coefficient ( $h_{sf}a_{sf}$  in equation 2) was set constant ( $200 \text{ W}(\text{m}^3\text{C})^{-1}$ ,  $Re = 0.0056$ ) in order to  
269 analyse only the effect of velocity on ATD (and neglect the effect of heat transfer coefficient).  
270 Figure 3 indicates that the lower the temperature amplitude applied at the top boundary the  
271 lower the resultant ATD. Moreover, the increase in velocity gives rise to increasing values for  
272 ATD particularly when it passes the threshold of  $Pe = 0.0074$  (or  $Re=0.01$ ). This is due to the  
273 fact that an increase in velocity leads to a higher localised temperature gradient at the grain  
274 boundary; greater thermal non-equilibrium occurs in these modelled conditions as conduction  
275 into the grains cannot keep pace with the advective flux of heat through the fluid (i.e. higher  
276 grain  $Pe$ ).

277

### 278 3.3 Error in derived streambed fluid velocity when assuming local thermal equilibrium

279 The relative ( $\frac{v_{ARorPS} - v_{actual}}{v_{actual}}$ ) and absolute ( $v_{ARorPS} - v_{actual}$ ) errors in pore water velocity (from  
280 both the AR and PS [8]) using  $T_s$ , or  $T_f$  as a function of  $Pe$  are presented in **Figure 4a-d**. From  
281 Fig. 4, the errors in derived velocity estimates converge to zero value for all cases as  $Pe$   
282 increases whether using  $T_s$ , or  $T_f$  except the  $PS$  velocity errors obtained from  $T_f$  and high solid  
283 thermal conductivity ( $k_{high}$ ). So, while the increase in advective flux ( $Pe$ ) tends to thermally  
284 disequilibrate the system (Fig. 3), this is more than compensated by an increased heat transfer  
285 coefficient ( $h_{sf}$ ) at higher velocities which tends to increase equilibrium between phases, leading  
286 to more equilibrium at higher  $Pe$  ( $Re$ ) in the range considered here (This is summarised  
287 conceptually in **Fig. 7**).

288 It can be seen from Fig. 4 that the AR derived relative and absolute velocity errors are negative  
289 and decrease with depth using  $T_f$  and high solid thermal conductivity ( $k_{high}$ ) at low  $Pe$  (low  $Re$ ),  
290 whereas the errors are positive using  $T_s$  with the same  $k_{high}$  and at low  $Pe$ . This is attributed to

291 the fact that  $AR$  values of the solid and fluid phases are different to that of the local thermal  
292 equilibrium case (i.e.  $AR$  derived from the 1-D analytical solution based on the LTE  
293 assumption). In order to compare the  $AR$  values of the numerical analysis to that of the  
294 analytical solution at different  $Re$  ( $=2.5 \times 10^{-4}$  and  $7.5 \times 10^{-4}$ ) **Fig. 5** is presented (it should be  
295 noted that  $Pe$  is replaced with  $Re$  in Fig. 5 due to the fact that  $Pe$  varies with change in solid  
296 thermal conductivity).

297

298 As an example, the  $AR$  values of the solid phase, with high solid thermal conductivity ( $k_{high}$ ) at  
299 low  $Pe$  ( $Re=2.5 \times 10^{-4}$ ), are higher than that of the local thermal equilibrium case leading to  
300 higher derived velocities than for the LTE case and thus positive errors.  $AR$  values of the fluid  
301 phase, with high solid thermal conductivity ( $k_{high}$ ) at low  $Pe$  ( $Re=2.5 \times 10^{-4}$ ), are lower leading to  
302 lower velocities than the LTE case and thus negative errors. It can also be seen from Fig. 2 that  
303 the temperature fluctuations of the LTE case is lower than the temperature fluctuations of the  
304 solid phase with  $k_{high}$  and higher than the temperature fluctuations of the fluid at low  $Pe$   
305 ( $Re=2.5 \times 10^{-4}$ ). The physical basis for these deviations is that at low  $Pe$ , the heat exchange  
306 between phases becomes inefficient and therefore, using  $k_{high}$ , the heat transport in the solid  
307 phase becomes much quicker than that within the fluid.

308

309 Using a lower solid thermal conductivity ( $k_{low}$ ) and low  $Pe$  ( $Re=2.5 \times 10^{-4}$ ), on the other hand, the  
310  $ARs$  using either  $T_s$  or  $T_f$  are both greater than those for the local thermal equilibrium case and  
311 therefore positive velocity errors are obtained. Again it can be explained by the fact that at low  
312  $Pe$  the heat exchange between phases is inefficient and since the solid thermal conductivity is  
313 low (very close to fluid thermal conductivity) the solid and fluid phases end up behaving  
314 similarly. The reason why the  $AR$  value of the LTE case is slightly lower than both the solid and  
315 fluid  $ARs$  is because of the difference in the thermal diffusivity of each phase and that of the  
316 LTE case. Although the thermal conductivity of the LTE case sits between the solid and fluid  
317 thermal conductivities, its thermal diffusivity may sit between or below the solid and thermal  
318 phases due to a different volumetric heat capacity. And because the thermal diffusivity affects  
319 the rate of heat transfer, lower magnitude of  $AR$  is observed compared to that of solid and fluid  
320 (where the thermal diffusivity of LTE case sits below the solid and thermal phases). It is  
321 noteworthy that the diffusivity is the function of both the thermal conductivity and the

322 volumetric heat capacity. When moving toward higher  $Pe$  ( $Re=7.5\times 10^{-4}$ ), the error approaches  
323 zero showing that the system reaches local thermal equilibrium.

324

325 The relative errors in the  $PS$  derived velocity estimates (Fig. 4) have similar trends and greater  
326 magnitudes compared to those derived using  $ARs$  especially at lower end of  $Pe$ . From Fig. 4d, it  
327 can be seen that the  $PS$  derived absolute velocity errors stay constant at relatively lower  
328 velocities ( $Pe$ ). Thus the relative errors increase only due to a reduction in the actual pore water  
329 velocity. Due to the fact that the  $AR$  and  $PS$  methods are sensitive to different velocities [8], the  
330  $PS$  method loses its sensitivity at lower range of velocity and the same velocity estimate is  
331 returned. In addition, the errors at higher velocities do not converge to the absolute zero which is  
332 resulted from the effect of local thermal non-equilibrium on the phase shift of the temperature  
333 data. The obtained  $PS$  values of the numerical analysis and analytical solution at different  $Re$   
334 ( $=2.5\times 10^{-4}$  and  $7.5\times 10^{-4}$ ) are also presented in **Fig. 6** for comparison.

335

336 Since the errors we have reported here are significant, especially for relatively low  $Pe$  (relative  
337 errors up to 30 and 150 are obtained from  $AR$  and  $PS$ ), we have compared the parameter range  
338 of our results to laboratory studies which present data with which it is possible to assess the  
339 robustness of a single-domain equation (implicitly assuming the validity of LTE) in deriving  
340 stream bed velocities using diurnal temperature signals. Surprisingly, given the ever increasing  
341 number of field applications using such an approach there are, to our knowledge, only 3  
342 laboratory studies of relevance. Rau et al. [19] found generally good agreement between  
343 experimental and theoretical expectations in a study conducted at a range of  $Re$  above the data  
344 presented here, in the range where we would expect the LTE assumption to be valid. Munz et  
345 al. [38] and Lautz [39] present results which may cross over with the range of  $Re$  we have  
346 analysed here although, unfortunately, neither paper is explicit regarding the grain size  
347 distribution used in their experiments. However, using a typical range of grain sizes for fine  
348 sand [39] and medium sand [38] the minimum  $Re$  studied may have been approximately  $6\cdot 10^{-3}$   
349 and  $2.5\cdot 10^{-3}$  respectively which are within the range of values where we would expect LTE to  
350 breakdown. In the Lautz [39] experiments, we note that significant discrepancies were found  
351 between velocities derived using  $AR$  and  $PS$ , which remain unexplained and that might be due to  
352 LTNE, although other effects such as heterogeneity can also induce such discrepancies [40, 41].

353 In the Munz et al. [38] experiments, increasing discrepancies are apparent between the measured  
354 and modelled flow velocities as the flow rate decreases. These observations are consistent with  
355 the understanding of LTNE described in this paper, and we propose that false assumptions of  
356 LTE may have contributed to these reported errors.

357 The errors that could arise due to a false assumption of LTE may be of the same order of  
358 magnitude as errors due to other factors such as non-uniform flow fields [10, 11], sediment  
359 heterogeneity [12], measurement error and difficulties in estimating thermal parameters [13, 14].

360

#### 361 **4. Conclusion**

362 Despite a large body of literature describing the fundamentals of heat transfer in porous media,  
363 the plethora of studies which have applied heat as a tracer in streambeds have, to our knowledge  
364 without exception, assumed local thermal equilibrium between solid and fluid phases. However,  
365 there is evidence from existing theory and empirical evidence that this assumption may not be  
366 valid in many instances [22, 28].

367 Here we have derived a correlation for the heat transfer coefficient at low  $Re$  using well known  
368 experimental data (KSC) which is in good agreement with a physically based model (NGM).

369 Our analysis reveals that two main mechanisms control the degree of thermal equilibrium  
370 between the solid and fluid phases in a typical streambed: the ratio of the conductive to  
371 advective heat transport (described by the grain thermal  $Pe$ ) and the heat transfer coefficient  
372 which is related to the  $Re$  (Figure 7). These processes act against each other; higher advection  
373 tends towards disequilibrium between phases while at high velocities this process is more than  
374 outweighed by an increasing heat transfer coefficient which tends to move the system towards  
375 equilibrium. Including these processes in a two-domain heat transport model we have shown

376 that the LTE assumption may break down at  $Re < 0.01$  for typical streambed thermal parameters.

377 Furthermore, this model output was then inverted using a 1D analytical model which assumes

378 LTE, to show that considerable relative errors in streambed velocity estimates may result at low  
379  $Re$  (or  $Pe$ ) if the possibility of LTNE is ignored. In general, these errors are higher at relatively

380 lower  $Re$  and may lead to significant inferred flows from data inversions based on the LTE  
381 assumption (0.3 m/d using  $AR$  and 1.3 m/d using  $PS$ ) when in fact the real flow is small or zero.

382 Such errors may be of the same order of magnitude as other known uncertainties in streambed  
383 heat tracing [10-14].



384 These results have important implications for interpreting and predicting streambed temperature  
385 dynamics, critical for improving the understanding of controls on stream ecology and  
386 biogeochemical processes. More laboratory studies are urgently needed to supplement the  
387 sparse existing data in this area and further test the findings of this study. In particular, the data  
388 and models on which this study is based was for homogeneous media and diel temperature  
389 signals, and it is to be expected that results will significantly differ for real field conditions; such  
390 data are required to enable a more complete physical understanding of heat transport processes  
391 in real streambeds to be derived.

392

### 393 **Acknowledgments**

394 Funding for this research was provided by the National Centre for Groundwater Research and  
395 Training, an Australian Government initiative, supported by the Australian Research Council  
396 and the National Water Commission. Mark Cuthbert acknowledges funding by the European  
397 Community's Seventh Framework Programme [FP7/2007-2013] under grant agreement  
398 n°299091.

399

400

401

402

403

404

405

406

407

408

409

410

411

412

413

414



415 **Appendix A**

416

417 **Table A.** Details of fitting parameters to the experimental data of Kunii and Smith [1961] in

418 Figure 1 using DATAFIT software.

Results from project "LTNE"	
Model Definition:	$Nu/Pr^2 = a+b*Re^c$ Where $a= \alpha/Pr^2$ , $b=K_1 \times Pr^{(1/3)}/Pr^2$ and $c=q$
Number of observations	41
Number of missing observations	0
Solver type	Nonlinear
Nonlinear iteration limit	250
Diverging nonlinear iteration limit	10
Number of nonlinear iterations performed	61
Residual tolerance	1.00E-10
Sum of Residuals	9.31E-15
Average Residual	2.27E-16
Residual Sum of Squares (Absolute)	3.63E-11
Residual Sum of Squares (Relative)	3.63E-11
Standard Error of the Estimate	9.78E-07
Coefficient of Multiple Determination (R <sup>2</sup> )	8.37E-01
Proportion of Variance Explained	83.68%
Adjusted coefficient of multiple determination (Ra <sup>2</sup> )	0.83
Durbin-Watson statistic	1.53

419

420

421

422

423

424

425 **Table B.** Regression variable results for the experimental data of Kunii and Smith [1961]  
 426 including the best fit and confidence intervals of 68%, 90%, 95% and 99% from DATAFIT  
 427 software.

Variable	Value	Standard	t-ratio	Prob(t)
A	7.35E-07	4.48E-07	1.640975375	0.10906
B	15.3962065	42.61194092	0.361312021	0.71987
C	2.687445266	0.51686944	5.199466357	0.00001
<b>68% Confidence</b>				
Variable	Value	68% (+/-)	Lower	Upper
A	7.35E-07	4.51E-07	2.84E-07	1.19E-06
B	15.3962065	42.93579167	-	58.33199817
C	2.687445266	0.520797648	2.166647618	3.208242914
<b>90% Confidence</b>				
Variable	Value	90% (+/-)	Lower	Upper
A	7.35E-07	7.55E-07	-2.02E-08	1.49E-06
B	15.3962065	71.84373239	-	87.23993889
C	2.687445266	0.871441876	1.816003389	3.558887142
<b>95% Confidence</b>				
Variable	Value	95% (+/-)	Lower	Upper
A	7.35E-07	9.07E-07	-1.72E-07	1.64E-06
B	15.3962065	86.2636132	-70.8674067	101.6598197
C	2.687445266	1.046350495	1.641094771	3.73379576
<b>99% Confidence</b>				
Variable	Value	99% (+/-)	Lower	Upper
A	7.35E-07	1.21E-06	-4.80E-07	1.95E-06
B	15.3962065	115.5422778	-	130.9384843
C	2.687445266	1.401491487	1.285953778	4.088936753
<b>Variance Analysis</b>				
Source	DF	Sum of	Mean	F Ratio
Regression	2	1.86E-10	9.32E-11	97.42871476
Error	38	3.63E-11	9.56E-13	
Total	40	2.23E-10		

428

429

430

431

432

433 **Appendix B**

434 *Numerical discretization:* the standard and Characteristic Galerkin techniques are used to  
 435 discretize the governing equations of the two-domain heat transport problem (equations 1 and  
 436 2). It results in the following system of equations for a two dimensional problem:

$$437 \quad [-(M + \Delta t[H - M_3])][\Delta \vec{T}_i^s] = [\Delta t[H - M_3]T_i^s(t_{i-1}) - \Delta t M_3 T_i^f(t_i)]$$

$$438 \quad [-(M + \Delta t(C - K_1 - K_2) - \Delta t M_2)][\Delta \vec{T}_i^f] = [\Delta t[(C - K_1 - K_2) - M_2]T_i^f(t_{i-1}) + \Delta t M_2 T_i^s(t_i)]$$

439

440 where  $i$  is the time step;  $\vec{T}$  is the temperature vector;  $\vec{T}_T = (T_1 \ T_2 \ \dots \ T_n)$ ;  $T$  is the nodal  
 441 temperature; subscripts s and f represent the solid and fluid phases respectively;  $\Delta t$  represents  
 442 the time increment and the matrices are defined as:

$$443 \quad \vec{M} = \int_{V_e} [N_T]^T [N_T] dV$$

$$444 \quad \vec{C} = \int_{V_e} [N_T]^T \frac{\partial}{\partial x} \left( \frac{1}{\phi} \left( \frac{\langle k \rangle^f}{\rho c_p} + f(\vec{\beta}, \vec{v}_x) \right) \frac{\partial [N_T]}{\partial x} \right) \{\chi\}^n dV + \int_{V_e} [N_T]^T \frac{\partial}{\partial y} \left( \frac{1}{\phi} \left( \frac{\langle k \rangle^f}{\rho c_p} + f(\vec{\beta}, \vec{v}_y) \right) \frac{\partial [N_T]}{\partial y} \right) \{\chi\}^n dV$$

$$445 \quad \vec{K}_1 = v_x^d \int_{V_e} [N_T]^T \frac{\partial [N_T]}{\partial x} \{\chi\}^n dV + v_y^d \int_{V_e} [N_T]^T \frac{\partial [N_T]}{\partial y} \{\chi\}^n dV$$

$$446 \quad \vec{K}_2 = \frac{\Delta t}{2} v_x^d \int_{V_e} \left[ \frac{\partial}{\partial x} \left( v_x^d \frac{\partial [N_T]}{\partial x} \{\chi\}^n + v_y^d \frac{\partial [N_T]}{\partial y} \{\chi\}^n \right) \right] dV + \frac{\Delta t}{2} v_y^d \int_{V_e} \left[ \frac{\partial}{\partial y} \left( v_x^d \frac{\partial [N_T]}{\partial x} \{\chi\}^n + v_y^d \frac{\partial [N_T]}{\partial y} \{\chi\}^n \right) \right] dV$$

$$447 \quad \vec{M}_2 = \int_{V_e} \frac{h_{sf} a_{sf}}{\phi (\rho c_p)_f} [N_T]^T [N_T] dV$$

$$448 \quad \vec{M}_3 = \int_{V_e} \frac{h_{sf} a_{sf}}{(1-\phi)(\rho c_p)_s} [N_T]^T [N_T] dV$$

$$449 \quad \vec{H} = \int_{V_e} [N_T]^T \frac{\partial}{\partial x} \left( \frac{\langle k \rangle^s}{(1-\phi)(\rho c_p)_s} \frac{\partial [N_T]}{\partial x} \right) \{\chi\}^n dV + \int_{V_e} [N_T]^T \frac{\partial}{\partial y} \left( \frac{\langle k \rangle^s}{(1-\phi)(\rho c_p)_s} \frac{\partial [N_T]}{\partial y} \right) \{\chi\}^n dV$$

450 where  $N_T$  is the finite element shape function of temperature,  $V$  is the spatial area of an element  
 451 and  $\chi$  is the variable.

452

453

454

455

456 **References**

- 457 [1] Krause S, DM Hannah, JH Fleckenstein, CM Heppell, D Kaeser, R Pickup, et al. Inter-  
458 disciplinary perspectives on processes in the hyporheic zone. *Ecohydrology*. 4 (2011) 481-99,  
459 doi: 10.1002/eco.176.
- 460 [2] Kaplan LA, TL Bott. Diel fluctuations in bacterial activity on streambed substrata during  
461 vernal algal blooms: Effects of temperature, water chemistry, and habitat *Limnol Oceanogr*. 34  
462 (1989) 118-733.
- 463 [3] Evans EC, GE Petts. Hyporheic temperature patterns within riffles. *Hydrological Sciences*  
464 *Journal*. 42 (1997) 199-213, doi: 10.1080/02626669709492020.
- 465 [4] Brunke M, TOM Gonser. The ecological significance of exchange processes between rivers  
466 and groundwater. *Freshwater Biology*. 37 (1997) 1-33, doi: 10.1046/j.1365-2427.1997.00143.x.
- 467 [5] Constantz J. Heat as a tracer to determine streambed water exchanges. *Water Resources*  
468 *Research*. 44 (2008) W00D10, doi: 10.1029/2008WR006996.
- 469 [6] Stallman RW. Steady One-Dimensional Fluid Flow in a Semi-Infinite Porous Medium with  
470 Sinusoidal Surface Temperature. *J Geophys Res*. 70 (1965) 2821-7, doi:  
471 10.1029/JZ070i012p02821.
- 472 [7] Keery J, A Binley, N Crook, JWN Smith. Temporal and spatial variability of groundwater-  
473 surface water fluxes: Development and application of an analytical method using temperature  
474 time series. *Journal of Hydrology*. 336 (2007) 1-16, doi: 10.1016/j.jhydrol.2006.12.003.
- 475 [8] Hatch CE, AT Fisher, JS Revenaugh, J Constantz, C Ruehl. Quantifying surface water-  
476 groundwater interactions using time series analysis of streambed thermal records: Method  
477 development. *Water Resour Res*. 42 (2006) W10410, doi: 10.1029/2005wr004787.
- 478 [9] Wörman A, J Riml, N Schmadel, BT Neilson, A Bottacin-Busolin, JE Heavilin. Spectral  
479 scaling of heat fluxes in streambed sediments. *Geophysical Research Letters*. 39 (2012) L23402,  
480 doi: 10.1029/2012GL053922.
- 481 [10] Cuthbert MO, R Mackay. Impacts of nonuniform flow on estimates of vertical streambed  
482 flux. *Water Resources Research*. 49 (2013) 19-28, doi: 10.1029/2011WR011587.
- 483 [11] Roshan H, GC Rau, MS Andersen, IR Acworth. Use of heat as tracer to quantify vertical  
484 streambed flow in a two-dimensional flow field. *Water Resources Research*. 48 (2012) W10508,  
485 doi: 10.1029/2012WR011918.
- 486 [12] Ferguson G, V Bense. Uncertainty in 1D Heat-Flow Analysis to Estimate Groundwater  
487 Discharge to a Stream. *Ground Water*. 49 (2011) 336-47, doi: 10.1111/j.1745-  
488 6584.2010.00735.x.
- 489 [13] Shanafield M, C Hatch, G Pohll. Uncertainty in thermal time series analysis estimates of  
490 streambed water flux. *Water Resour Res*. 47 (2011) W03504, doi: 10.1029/2010wr009574.
- 491 [14] Cuthbert MO, R Mackay, V Durand, MF Aller, RB Greswell, MO Rivett. Impacts of river  
492 bed gas on the hydraulic and thermal dynamics of the hyporheic zone. *Advances in Water*  
493 *Resources*. 33 (2010) 1347-58, doi: <http://dx.doi.org/10.1016/j.advwatres.2010.09.014>.
- 494 [15] Nield DA, A Bejan. *Convection in Porous Media*. Third Edition ed. SPRINGER, 2006.
- 495 [16] Kaviany M. *Principles of Heat Transfer in Porous Media*. 2nd ed. Springer, 1995.
- 496 [17] Amiri A, K Vafai. Analysis of dispersion effects and non-thermal equilibrium, non-  
497 Darcian, variable porosity incompressible flow through porous media. *International Journal of*  
498 *Heat and Mass Transfer*. 37 (1994) 939-54, doi: 10.1016/0017-9310(94)90219-4.
- 499 [18] Alazmi B, K Vafai. Analysis of Variable Porosity, Thermal Dispersion, and Local Thermal  
500 Nonequilibrium on Free Surface Flows Through Porous Media. *Journal of Heat Transfer*. 126  
501 (2004) 389-99.

- 502 [19] Rau GC, MS Andersen, RI Acworth. Experimental investigation of the thermal dispersivity  
503 term and its significance in the heat transport equation for flow in sediments. *Water Resour Res.*  
504 48 (2012) W03511, doi: 10.1029/2011wr011038.
- 505 [20] Vafai K, M Sozen. Analysis of Energy and Momentum Transport for Fluid Flow Through a  
506 Porous Bed. *Journal of Heat Transfer.* 112 (1990) 690-9.
- 507 [21] Wakao N, S Kaguei, T Funazkri. Effect of fluid dispersion coefficients on particle-to-fluid  
508 mass transfer coefficients in packed beds: Correlation of sherwood numbers. *Chemical*  
509 *Engineering Science.* 33 (1978) 1375-84, doi: 10.1016/0009-2509(78)85120-3.
- 510 [22] Nelson PA, TR Galloway. Particle-to-fluid heat and mass transfer in dense systems of fine  
511 particles. *Chemical Engineering Science.* 30 (1975) 1-6, doi: 10.1016/0009-2509(75)85109-8.
- 512 [23] Verschoor H, GCA Schuit. Heat transfer to fluids flowing through a bed of granular solids.  
513 *Appl sci Res.* 2 (1951) 97-119, doi: 10.1007/BF00411975.
- 514 [24] Gupta AS, G Thodos. Transitional Behavior for the Simultaneous Mass and Heat Transfer  
515 of Gases Flowing through Packed and Distended Beds of Spheres. *Industrial & Engineering*  
516 *Chemistry Fundamentals.* 3 (1964) 218-20, doi: 10.1021/i160011a008.
- 517 [25] McConnachie JTL, G Thodos. Transfer processes in the flow of gases through packed and  
518 distended beds of spheres. *AICHE Journal.* 9 (1963) 60-4, doi: 10.1002/aic.690090113.
- 519 [26] Wang W, J Li, W Wang, X Chen, D Cheng, J Jia. Estimating streambed parameters for a  
520 disconnected river. *Hydrological Processes.* (2013) accepted May 2013, doi: 10.1002/hyp.9904.
- 521 [27] Jensen JK, P Engesgaard. Nonuniform Groundwater Discharge across a Streambed: Heat as  
522 a Tracer. *Vadose Zone Journal.* 10 (2011) 98-109, doi: 10.2136/vzj2010.0005.
- 523 [28] Kunii D, JM Smith. Heat transfer characteristics of porous rocks: II. Thermal conductivities  
524 of unconsolidated particles with flowing fluids. *AICHE Journal.* 7 (1961) 29-34, doi:  
525 10.1002/aic.690070109.
- 526 [29] Jiang P-X, R-N Xu, W Gong. Particle-to-fluid heat transfer coefficients in miniporous  
527 media. *Chemical Engineering Science.* 61 (2006) 7213-22, doi: 10.1016/j.ces.2006.08.003.
- 528 [30] Cybulski A, MJ Van Dalen, JW Verkerk, PJ Van Den Berg. Gas-particle heat transfer  
529 coefficients in packed beds at low Reynolds numbers. *Chemical Engineering Science.* 30 (1975)  
530 1015-8, doi: 10.1016/0009-2509(75)87002-3.
- 531 [31] Ranz WE. Evaporation from drops: Part I. *Chem Engng Progr.* 48 (1952).
- 532 [32] Lienhard JH. *A Heat Transfer TextBook.* Third ed. Phlogiston Press, 2008.
- 533 [33] Scala F. Particle-fluid mass transfer in multiparticle systems at low Reynolds numbers.  
534 *Chemical Engineering Science.* 91 (2013) 90-101, doi:  
535 <http://dx.doi.org/10.1016/j.ces.2013.01.012>.
- 536 [34] Rowe PN. Particle-to-liquid mass transfer in fluidised beds. *Chemical Engineering Science.*  
537 30 (1975) 7-9, doi: [http://dx.doi.org/10.1016/0009-2509\(75\)85110-4](http://dx.doi.org/10.1016/0009-2509(75)85110-4).
- 538 [35] Farouki OT. Thermal properties of soils. U.S. Army Cold Regions Research and  
539 Engineering Laboratory 1981.
- 540 [36] Zienkiewicz O, R Taylor. *The finite element method, basic formulation and linear*  
541 *problems.* Butterworth-Heinemann, Oxford, 2000.
- 542 [37] Lewis RW, P Nithiarasu, KN Seetharamu. *Fundamentals of the Finite Element Method for*  
543 *Heat and Fluid Flow.* John Wiley 2004.
- 544 [38] Munz M, SE Oswald, C Schmidt. Sand box experiments to evaluate the influence of  
545 subsurface temperature probe design on temperature based water flux calculation. *Hydrology*  
546 *and Earth System Sciences.* 15 (2011) 3495-510.

547 [39] Lautz LK. Observing temporal patterns of vertical flux through streambed sediments using  
548 time-series analysis of temperature records. *Journal of Hydrology*. 464–465 (2012) 199-215,  
549 doi: <http://dx.doi.org/10.1016/j.jhydrol.2012.07.006>.

550 [40] Luce CH, D Tonina, F Gariglio, R Applebee. Solutions for the diurnally forced advection-  
551 diffusion equation to estimate bulk fluid velocity and diffusivity in streambeds from temperature  
552 time series. *Water Resources Research*. 49 (2013) 488-506, doi: 10.1029/2012WR012380.

553 [41] McCallum AM, MS Andersen, GC Rau, RI Acworth. A 1-D analytical method for  
554 estimating surface water-groundwater interactions and effective thermal diffusivity using  
555 temperature time series. *Water Resources Research*. 48 (2012) W11532, doi:  
556 10.1029/2012WR012007.

557

558

559

560

561

562

563

564

565

566

567

568

569

570

571

572

573

574

575

576

577

578

579

580

581 **Figure 1** Variation of  $Nu$  with  $Re$ : Kunii & Smith (1961) experimental data alongside our  
 582 correlation and the Nelson Galloway Model (NGM) results for a variety of porous material  
 583 porosities ( $\phi$ ).

584

585 **Figure 2** Sinusoidal temperature fluctuations at the surface and at 0.2 m depth for  $Re$  numbers  
 586 of  $7.5 \times 10^{-3}$  and  $2.5 \times 10^{-4}$  and high ( $2.4 \text{ W(mC)}^{-1}$ ) and low ( $0.8 \text{ W(mC)}^{-1}$ ) solid thermal  
 587 conductivities. Temperatures were calculated for the solid and the fluid by the two-domain  
 588 model (as outlined in the methodology), and for the assumption of local thermal equilibrium  
 589 (LTE) using the method by Hatch et al. [8] and for the case of no flow (thermal diffusion only).

590

591 **Figure 3.** the amplitude of the temperature difference (ATD) as a function of  $Re$  at four different  
 592 temperature amplitudes (1, 2, 3 and 4 °C) at the stream-sediment temperature boundary  
 593 condition. For this simulation the heat transfer coefficient has been held constant and the depth  
 594 of measurement is 0.2 m.

595

596 **Figure 4.** a)  $AR$  derived relative velocity error, b)  $PS$  derived relative velocity error c)  $AR$   
 597 derived absolute velocity error and d)  $PS$  derived absolute velocity error vs  $Pe_{avg}$  using solid and  
 598 fluid phase temperatures and higher and lower values of solid thermal conductivity ( $k_{s\_min}=0.8$   
 599  $\text{W(mC)}^{-1}$  and  $k_{s\_max}=2.4 \text{ W(mC)}^{-1}$ ). The velocity range is  $\sim 0.01\text{-}0.3$  m/d. For all plots the set of  
 600 curves for each symbol represents velocity error estimates for depths of 0.1, 0.2, 0.3, 0.35, 0.4  
 601 and 0.45 m.

602

603 **Figure 5.** The amplitude ratio ( $AR$ ) of the temperature signal vs depth at high ( $=7.5 \times 10^{-3}$ ) and  
 604 low ( $=2.5 \times 10^{-4}$ ) Reynolds numbers for high and low solid thermal conductivities using solid and  
 605 fluid temperatures. Also shown are the  $AR$ s derived using the 1-D analytical solution which  
 606 assumes LTE [Hatch et al, 2006].

607

608 **Figure 6.** The phase shift ( $PS$ ) of the temperature signal ( $PS$ ) vs depth at high ( $=7.5 \times 10^{-3}$ ) and  
 609 low ( $=2.5 \times 10^{-4}$ ) Reynolds numbers for high and low solid thermal conductivities using solid and  
 610 fluid temperatures. Also shown are the  $PS$  derived using the 1-D analytical solution which  
 611 assumes LTE [Hatch et al, 2006].

612 **Figure 7.** The relative importance of advective heat transport through the fluid, and heat  
613 transfer between the solid and the fluid phases at high and low  $Re$ . a) At low flow rates the heat  
614 transfer is relatively inefficient at thermally equilibrating the solid and fluid phases and LNTE is  
615 possible. b) At high rates of fluid advection (high  $Pe$ ) even though heat is advected fast through  
616 the porous media the heat transfer is far more efficient and helps maintain LTE.

617

618 **Table 1.** Physical data used in the study.

619

620

621

622

623

624

625

626

627

628

629

630

631

632

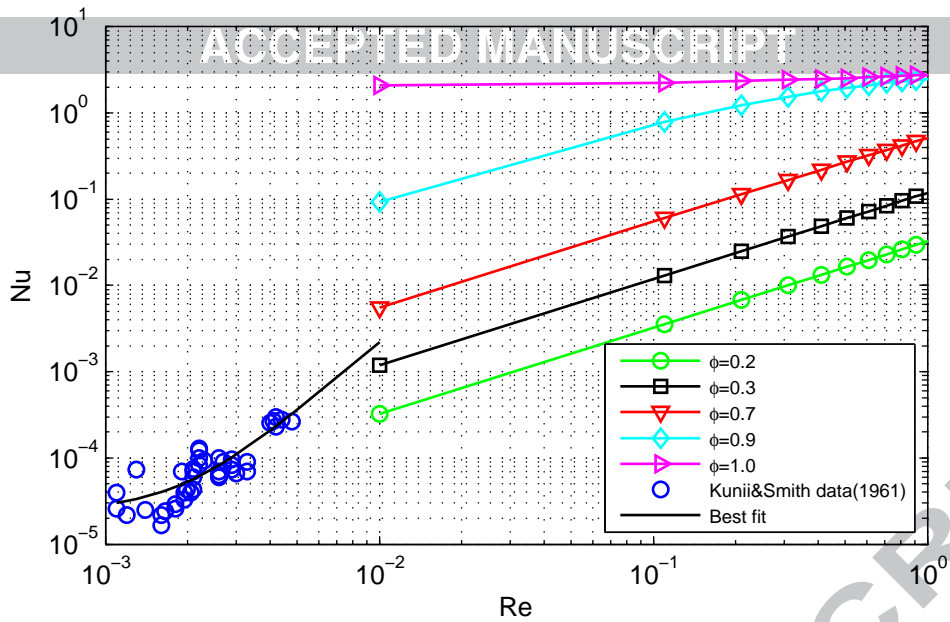
633

634

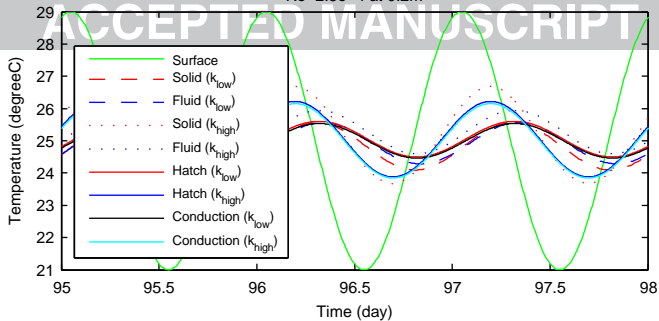
635

636

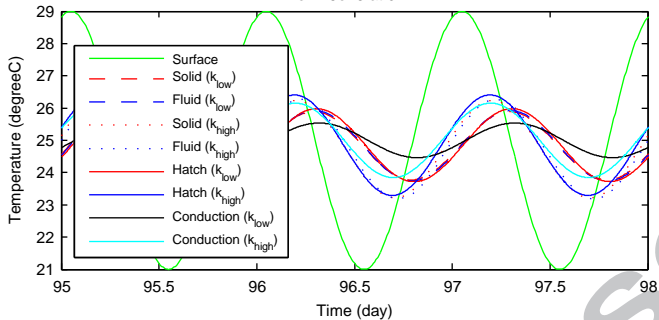


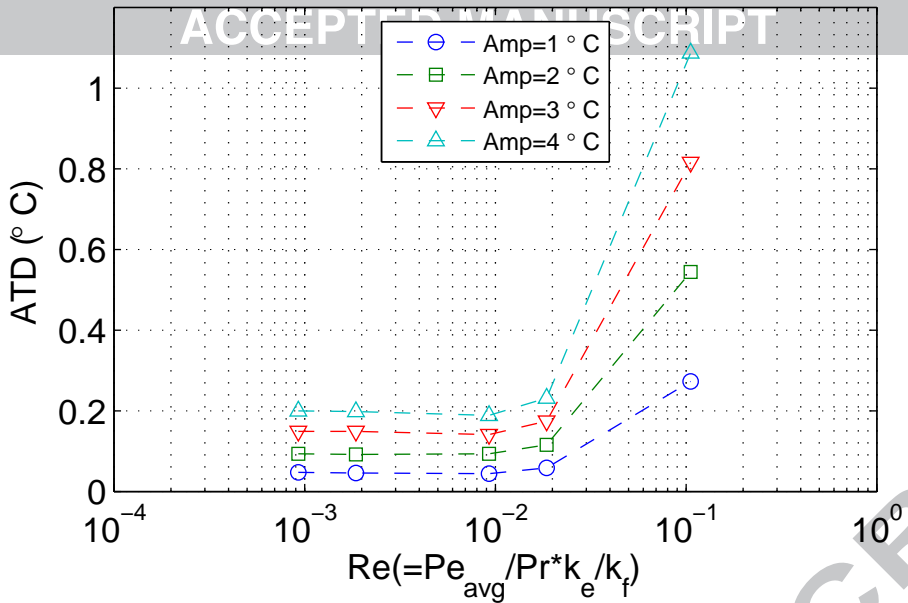


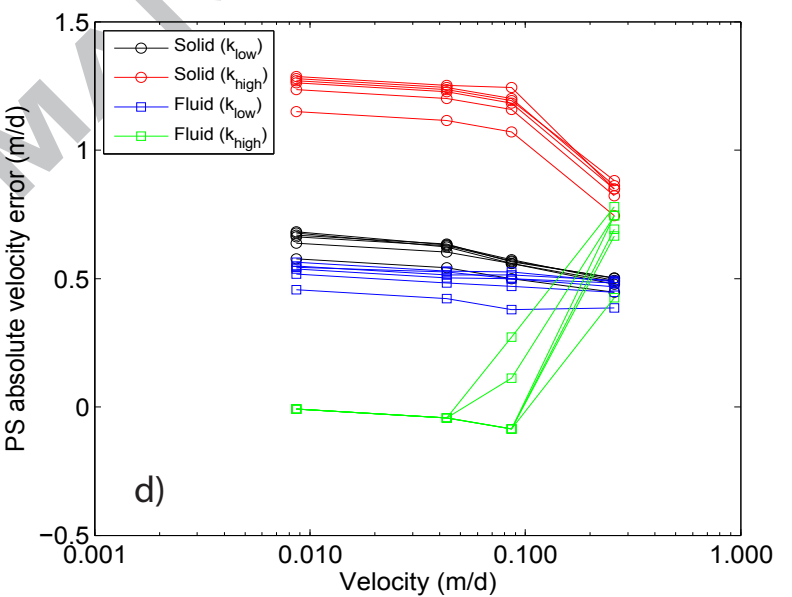
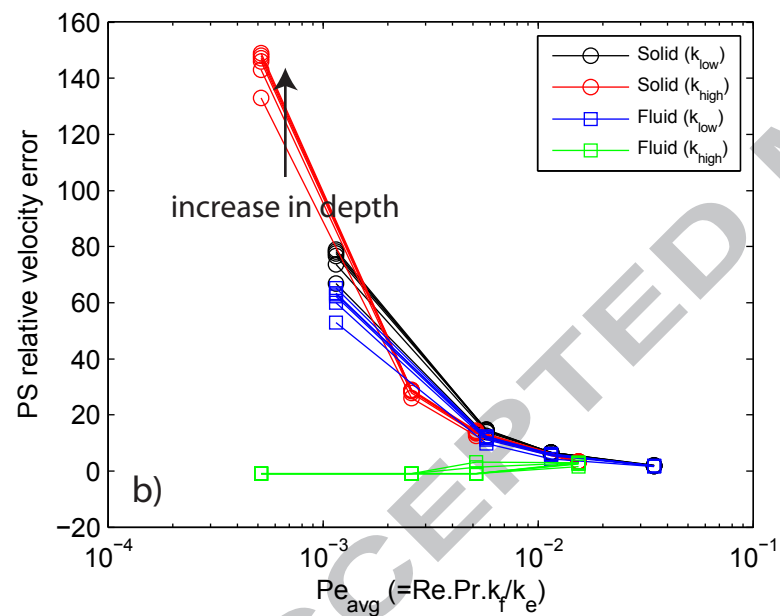
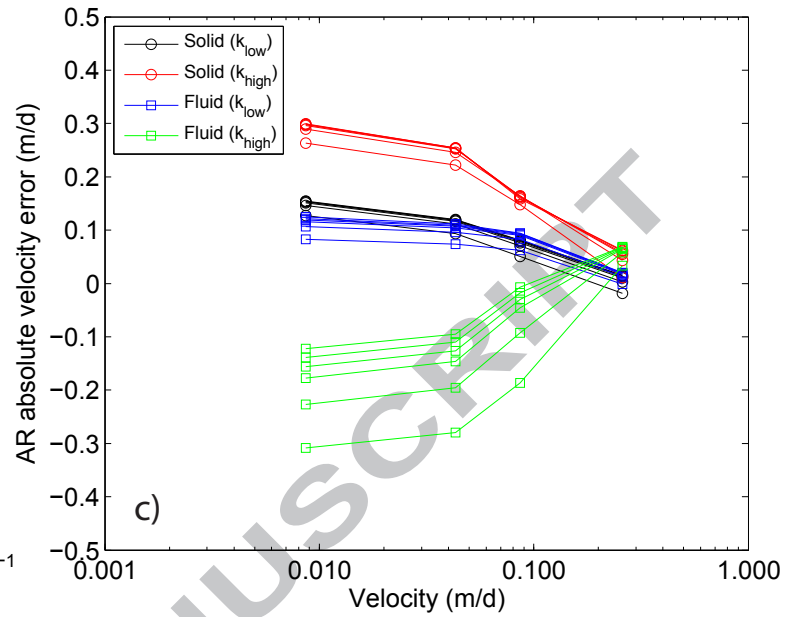
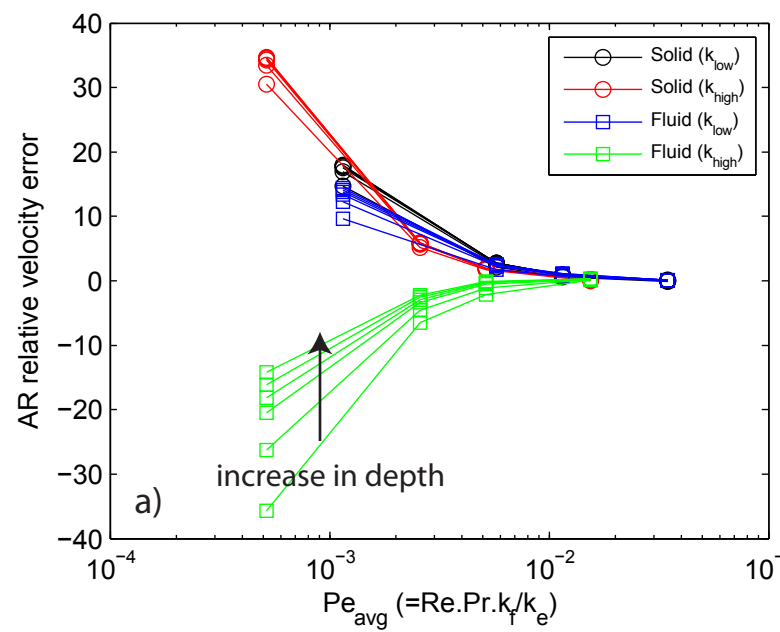
Re=2.5e-4 at 0.2m



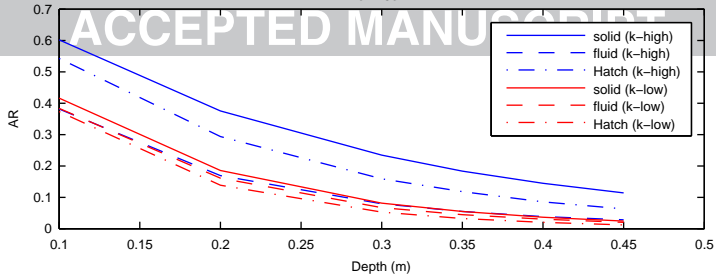
Re=7.5e-3 at 0.2m



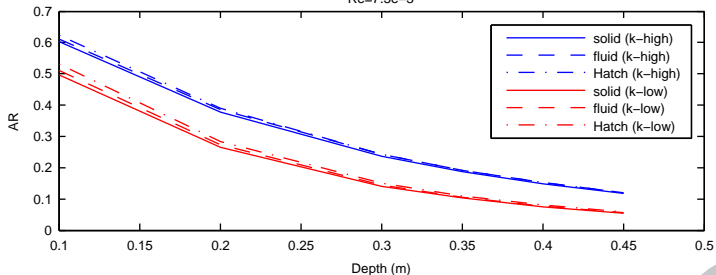


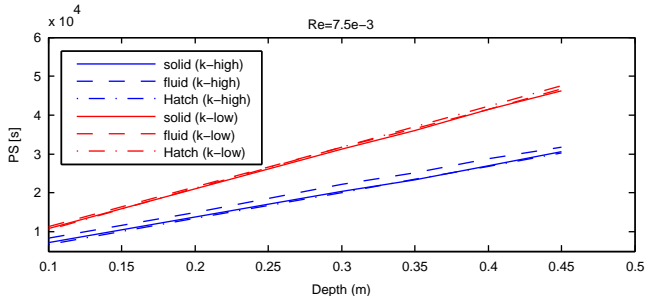
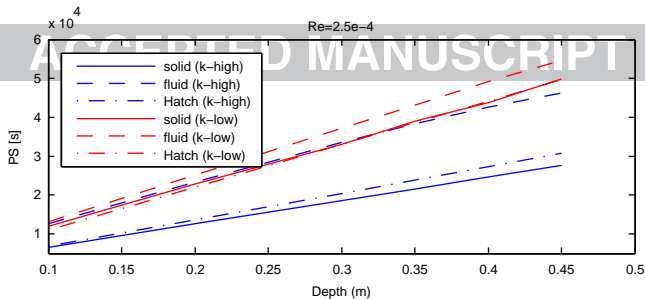


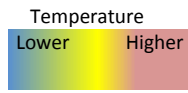
Re=2.5e-4



Re=7.5e-3

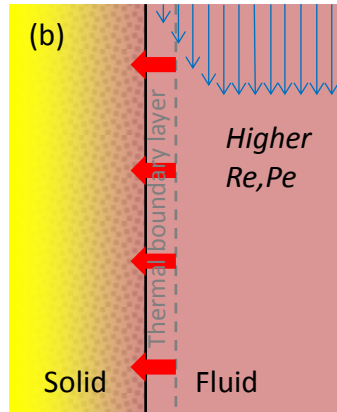
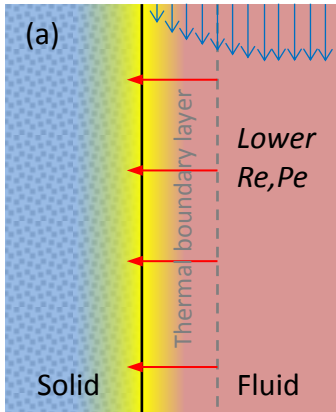






Relative rate of fluid-solid heat exchange

Relative rate of fluid advection



637 Table 1

Parameter	Unit	Symbol	Value
Solid Thermal Conductivity	$W(mC)^{-1}$	$k_{s\_min} \& k_{s\_min}$	0.8 & 2.5
Water Thermal Conductivity	$W(mC)^{-1}$	$k_f$	0.58
Water Specific Heat Capacity	$J(kgC)^{-1}$	$c_f$	4183
Solid Specific Heat Capacity	$J(kgC)^{-1}$	$c_s$	750
Water Density	$kg\ m^{-3}$	$\rho_f$	999.7
Solid Density	$kg\ m^{-3}$	$\rho_s$	2650
Porosity	-	$\phi$	0.3
Longitudinal Thermal Dispersivity	s	$\beta_l$	1.478
Transverse Thermal Dispersivity	s	$\beta_t$	0.4

638

639



640 **Highlights**

- 641 • We have derived a correlation for heat transfer coefficient at low  $Re$
- 642 • Local thermal equilibrium may not be a valid assumption in sediments' heat transfer
- 643 • Error in temperature derived velocity estimates may be obtained using LTE

644

645

ACCEPTED MANUSCRIPT